Synthesis, in vitro, and in vivo biological evaluation and molecular docking simulations of chiral alcohol and ether derivatives of the 1,5-diarylpyrrole scaffold as novel anti-inflammatory and analgesic agents

Mariangela Biava [a,*], Giulio C. Porretta [a], Giovanna Poce [a], Sibilla Supino [a], Fabrizio Manetti [b,*], Stefano Forli [b], Maurizio Botta [b], Lidia Sautebin [d], Antonietta Rossi [d,e], Carlo Pergola [d], Carla Ghelardini [f], Monica Norcini [f], Francesco Makovec [g], Antonio Giordani [g], Paola Anzellotti [h], Roberto Cirilli [i], Rosella Ferretti [i], Bruno Gallinella [i], Francesco La Torre [i], Maurizio Anzini [b,c], Paola Patrignani [h]

[a] *Dipartimento di Studi di Chimica e Tecnologie del Farmaco, Università 'La Sapienza', Piazzale Aldo Moro, 5, I-00185 Roma, Italy*
[b] *Dipartimento Farmaco Chimico Tecnologico, Università degli Studi di Siena, Via Alcide de Gasperi 2, I-53100 Siena, Italy*
[c] *European Research Centre for Drug Discovery and Development, via Banchi di Sotto 55, I-53100 Siena, Italy*
[d] *Dipartimento di Farmacologia Sperimentale, Università di Napoli 'Federico II', via D. Montesano 49, I-80131 Napoli, Italy*
[e] *IRCCS Centro Neurolesi 'Bonino-Pulejo', Via Provinciale Palermo—C.da Casazza, I-98124 Messina, Italy*
[f] *Dipartimento di Farmacologia, Università di Firenze, viale G. Pieraccini 6, I-50139 Firenze, Italy*
[g] *Rottapharm S.p.A., via Valosa di Sopra 7, I-20052 Monza, Italy*
[h] *Department of Medicine and Center of Excellence on Aging, 'G. d'Annunzio' University and CeSI, Via dei Vestini 31, I-66013 Chieti, Italy*
[i] *Istituto Superiore di Sanità, Dipartimento del Farmaco, Viale Regina Elena 299, I-00161 Roma, Italy*

ARTICLE INFO

ABSTRACT

Following our previous research on anti-inflammatory drugs (NSAIDs), we report here the synthesis of chiral 1,5-diarylpyrroles derivatives that were characterized for their in vitro inhibitory effects toward cyclooxygenase (COX) isozymes. Analysis of enzymatic affinity and COX-2 selectivity led us to the selection of one compound (+/−)-**10b** that was further tested in vitro in the human whole blood (HWB) and in vivo for its anti-inflammatory activity in mice. The affinity data have been rationalized through docking simulations.

© 2008 Elsevier Ltd. All rights reserved.

1. Introduction

Nonsteroidal anti-inflammatory drugs (NSAIDs) [traditional tNSAIDs and NSAIDs selective for cyclooxygenase (COX)-2, named coxibs] are a chemically heterogeneous group of agents to treat symptoms of acute pain and chronic inflammatory and degenerative joint diseases, which act mainly through the inhibition of COX-2-dependent prostanoids.[1] However, they are associated with side-effects for the gastrointestinal (GI) (i.e., dyspepsia, ulcer, perforation, occlusion, and bleeding) and cardiovascular (CV) system (myocardial infarction, stroke, hypertension, sodium retention with edema and heart failure), which plausibly involve the inhibition of COX-1 and COX-2, respectively.[2–4]

Selectivity for COX-2 in vitro (a chemical property of a COX inhibitor) is described as the ratio of the concentrations required to inhibit the activity of the isozymes by 50% (IC_{50} for COX-1/IC_{50} for COX-2).[4] Using the whole blood assays in vitro, Patrignani P. et al. evidenced that the biochemical selectivity of COX inhibitors is a continuous variable.[5,6] It was shown that, among traditional tNSAIDs, there is a cluster of compounds, such as etodolac[7] (**2**), meloxicam[8] (**3**), nimesulide[9] (**4**), and diclofenac[10] (**5**, Chart 1), which are from 5- to 29-fold more potent toward COX-2 in vitro.
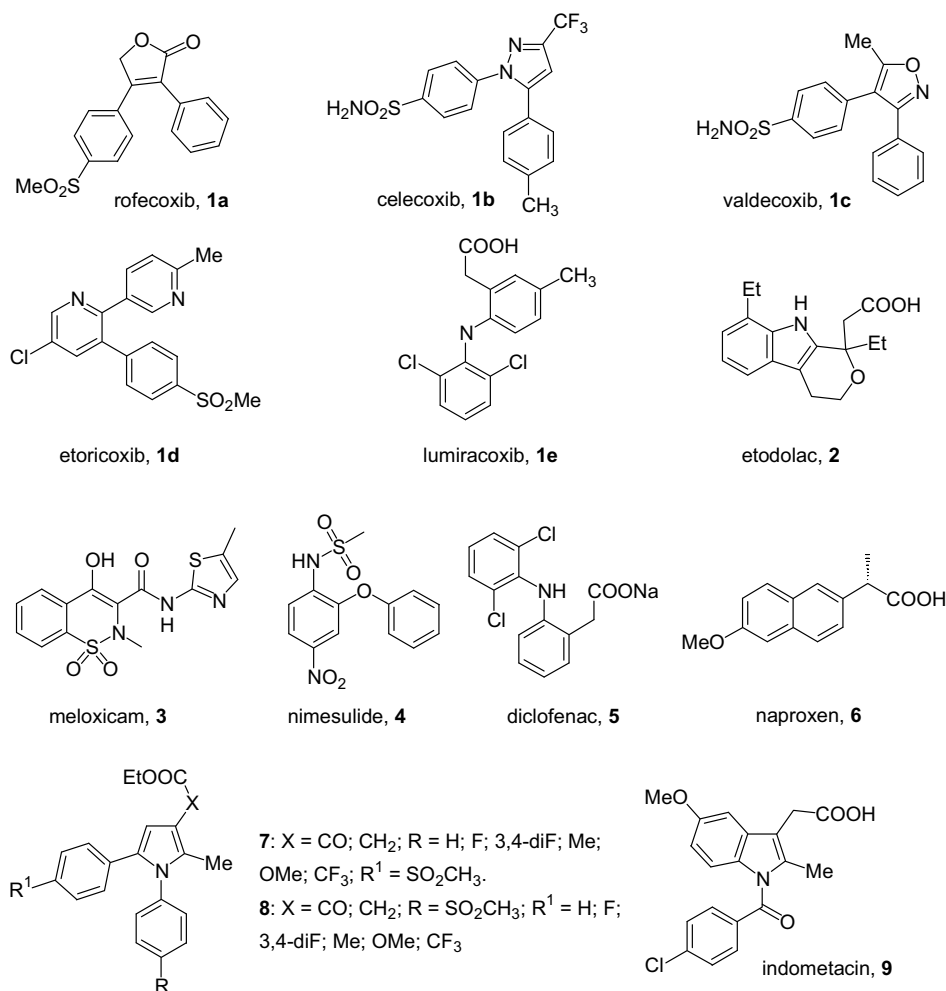
Chart 1. Chemical structure of NSAIDs: coxib derivatives, traditional NSAIDs and previous pyrrole compounds.

Among NSAIDs selective for COX-2 (commonly named coxibs: rofecoxib,[11] **1a**; celecoxib,[12] **1b**; valdecoxib,[13] **1c**; etoricoxib,[14] **1d**; and lumiracoxib,[15] **1e**, Chart 1), developed to reduce the incidence of serious GI effects, a wide spectrum of COX-1/COX-2 IC$_{50}$ ratio was reported, which ranges from 30 for **1b** to 433 for **1e**. However, efficacy and side-effects in vivo are dependent on the achieved selectivity (i.e., the ratio of degree of suppression of COX-1 and COX-2 at circulating drug concentrations), which is driven by pharmacokinetic features and dose-potency, but also influenced by marked variability in how each person reacts to these drugs based on its genetic background.[4,16]

It has been shown that 80% inhibition of COX-2 ex vivo (in whole blood) by circulating drug concentrations seems sufficient to translate into efficacy (analgesia).[17] High degrees of inhibition of COX-2 seem to be associated with increased incidence of vascular events (with myocardial infarction that exceeds over stroke), an effect that can be mitigated, but not obliterated, by complete and persistent (throughout dosing interval) inhibition of platelet COX-1 activity (i.e., >95%, necessary to inhibit platelet function).[3,4] Among tNSAIDs, only naproxen[18] (**6**, Chart 1), a balanced inhibitor of COX-1 and COX-2 with long half-life (>12 h), seems to have these pharmacokinetic and pharmacodynamic features.[19,20] Thus, most of tNSAIDs and coxibs are functionally selective for COX-2 in vivo in respect of the platelet COX-1, at therapeutic doses. This explains why coxibs but also some tNSAIDs are thrombogenic.[21,22] Differently from platelets, in the kidney, an incomplete inhibition

of COX-1 might attenuate the deleterious functional effect derived from inhibition of COX-2-dependent prostacyclin.[3,22] Thus, selective and profound inhibition of COX-2 by coxibs may have a greater propensity to increase blood pressure than concomitant inhibition of both COX-1 and COX-2 by tNSAIDs.

The results of human pharmacology and clinical trials have enlightened that a NSAID with 5- to 10-fold higher selectivity for COX-2 versus COX-1 in vitro might translate into acceptable GI safety profile when administered to a dose causing 70–80% inhibition of COX-2 ex vivo appropriate for efficacy. Presumably, this will leave sufficient COX-2-dependent generation of prostacyclin to sustain vascular function. Of course, this strategy will not obliterate the incidence of CV and GI toxicity in susceptible patients. The only way to reduce the incidence of these effects is by the development of genetic or biochemical biomarkers predictive of toxicity to select the individuals that should avoid the use of these pain killers.

Despite several NSAIDs with these pharmacodynamic features available (e.g., **3**–**5**), most of them have short half-life, which leads to their administration at high doses (often overshooting) to extend the pharmacodynamic effects, and importantly some are associated with hepatic toxicity (i.e., **5**). It should be pointed out that the Food and Drug Administration has recently rejected **1e** (a **5**-derived coxib) as a treatment for patients with osteoarthrosis pain. The coxib was recently withdrawn in Australia, placed under restrictions in the EU and undergoing review by Health Canada, following reports of serious liver damage. Thus, there is the need

to have novel NSAIDs with improved pharmacokinetic features and metabolism.

In the context of COX inhibitors, we recently reported several investigations describing the design, synthesis, and anti-inflammatory properties for a class of novel pyrrole-containing anti-inflammatory agents.[23,24] In particular, we focused our attention on the synthesis of 1,5-diarylpyrrol-3-acetic and -glyoxylic acid and esters **7** and **8** (Chart 1) as new COX-2 selective inhibitors in which the pyrroleacetic and vicinal diaryl heterocyclic moieties were reminiscent of both indomethacin[25] (**9**) and the above-cited 'coxib' family, respectively. A structure–activity relationship (SAR) analysis of such compounds, supported by molecular docking simulations of inhibitors into the COX-2 binding site, allowed us to rule out several considerations: (i) the position of the *p*-methylsulfonyl substituent was very important for activity, compounds **7** being more active than **8**, (ii) the acetic group at C3 of the pyrrole ring led to compounds more active than the corresponding glyoxylic analogues, (iii) substituents and substitution pattern on the phenyl ring at N1 influenced activity in the following order: 3-F > 4-F > 3,4-diF > 4-OMe > H > 4-CF$_3$ > 4-CH$_3$.[24] On this basis, we planned the synthesis of new derivatives, keeping the most convenient fluorine substitution (namely the 3-F substituent at the N1 phenyl ring, previously suggested by docking calculations), as well as the 4-methoxyphenyl group and an unsubstituted phenyl ring at position 1 of the pyrrole. On the other hand, a hydroxy or an ethoxy group was introduced into the methylene moiety of the C3 alkyl chain (leading to the corresponding alcohol and ether chiral derivatives **10a–c** and **11a–c**, respectively, Table 1) to investigate on the influence that different substituents at the α-position of this side chain could exert on the activity, and to check the possible variation of activity induced by different enantiomers.

We performed on all the new compounds a preliminary screening for COX-isozyme inhibition using a cell-based assay to identify the compounds with IC$_{50}$ values in the submicromolar range, com-

parable to that of the reference compound **1b**. Moreover, one of the most active compounds, (+/−)-**10b**, was also tested for its in vivo anti-inflammatory activity in the carrageenan-induced paw edema test. Finally, the human whole blood (HWB) in vitro assay was utilized to assess the pattern of the relative inhibition for platelet COX-1 and monocyte COX-2 by compound (+/−)-**10b** in comparison with the coxib **1b** and the tNSAID **2**.

2. Results and discussion

2.1. Chemistry

The synthesis of the target compounds is described in Scheme 1. Briefly, compounds **12a–c**, obtained by a procedure previously described,[23,24] were reduced with sodium cyanoborohydride in the presence of *tert*-butyl alcohol to give α-hydroxy pyrroleacetic ethyl esters **10a–c** as mixture of enantiomers, or with sodium cyanoborohydride in the presence of ethanol to give α-ethoxy pyrroleacetic ethyl esters **11a–c**, as mixture of enantiomers. Enantiomerically pure samples were obtained, at mg-scale, by HPLC on the amylose-based Chiralpak IA chiral stationary phase. In particular, the absolute configuration of (−)-**10b** was determined by single-crystal X-ray diffraction analysis. The molecular structure and the crystallographic data are reported elsewhere.[26] The findings of X-ray structure analysis allowed to assign unambiguously the (*R*)-configuration to the (−)-**10b** enantiomer. Then, the stereochemistry of remaining pyrrole derivatives was empirically assigned by circular dichroism spectroscopy.[26]

2.2. Biology

Compounds **10a–c** and **11a–c** were all evaluated for their anti-inflammatory activity toward both COX-2 and COX-1 enzymes following protocols previously described.[24]

Table 1
Structural properties and in vitro inhibition of COX-1 and COX-2 by compounds **10a–c**, **11a–c**, and **1b**
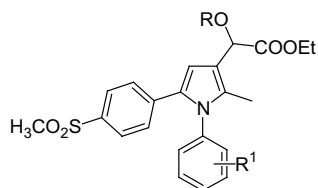
Compound	R	R^1	IC$_{50}$^{a} (µM)		% Inhibition		COX-1/COX-2^b (SI)
			COX-1	COX-2	COX-2 (10 µM)	COX-2 (1 µM)	
(+/−)-**10a**	H	H	>100	0.30	100	78	>600
(+)-(*S*)-**10a**	H	H	>100	0.18	92	79	>550
(−)-(*R*)-**10a**	H	H	>100	0.15	92	86	>650
(+/−)-**10b**	H	3-F	>100	0.12	100	70	>800
(+)-(*S*)-**10b**	H	3-F	>100	1.10	84	56	>90
(−)-(*R*)-**10b**	H	3-F	>100	0.075	92	86	>1300
(+/−)-**10c**	H	4-OMe	>100	0.12	100	82	>800
(+)-(*S*)-**10c**	H	4-OMe	>100	0.079	100	88	>1200
(−)-(*R*)-**10c**	H	4-OMe	>100	0.15	93	86	>650
(+/−)-**11a**	Et	H	>100	0.18	100	90	>800
(+)-(*S*)-**11a**	Et	H	>100	0.10	100	81	>1000
(−)-(*R*)-**11a**	Et	H	>100	0.14	86	77	>700
(+/−)-**11b**	Et	3-F	>100	0.10	100	74	>1000
(+)-(*S*)-**11b**	Et	3-F	>100	0.25	100	86	>400
(−)-(*R*)-**11b**	Et	3-F	>100	0.81	100	73	>100
(+/−)-**11c**	Et	4-OMe	>100	0.13	—	—	>800
(+)-(*S*)-**11c**	Et	4-OMe	>100	0.14	100	100	>700
(−)-(*R*)-**11c**	Et	4-OMe	>100	0.09	100	87	>1100
Celecoxib, **1b**			3.7	0.06	100	80	61.7

^{a} Results are expressed as the mean, for three experiments, of the % inhibition of PGE$_2$ production by test compounds with respect to control samples.
^{b} In vitro COX-2 Selectivity Index (IC$_{50(COX-1)}$/IC$_{50(COX-2)}$).
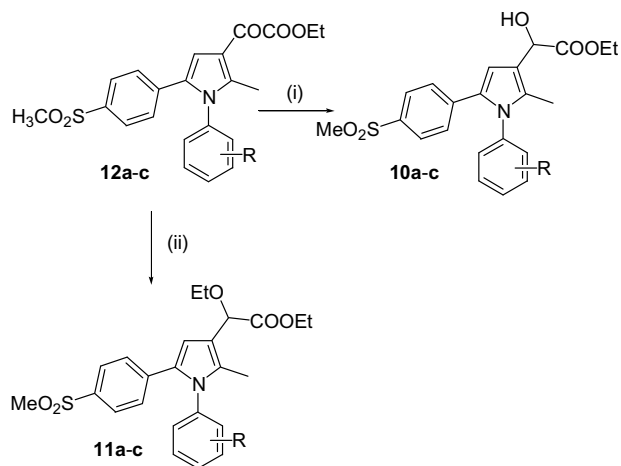
Scheme 1. Compounds: **10a**, R = H; **10b**, R = 3-F; **10c**, R = OMe; **11a**, R = H; **11b**, R = 3-F; **11c**, R = OMe; **12a**, R = H; **12b**, R = 3-F; **12c**, R = OMe. Reagents and conditions: (i) ZnCl$_2$, sodium cyanoborohydride, CH$_2$Cl$_2$, *tert*-butyl alcohol, rt, 2 h; (ii) ZnCl$_2$, CH$_2$Cl$_2$, ethyl alcohol, rt, 2 h.

Moreover, compound (+/−)-**10b** was also evaluated for COX-1 versus COX-2 selectivity by the use of the HWB assay, as reported elsewhere.[24] Its in vivo anti-inflammatory and analgesic activity was also checked on Male Swiss albino mice (23–25 g) and Sprague–Dawley or Wistar rats (150–200 g). In detail, the paw-pressure test, the carrageenan-induced paw edema test, and the abdominal writhing test were performed as previously reported.[24]

2.3. Results and discussion

Analysis of biological data from the cell-based assay showed IC$_{50}$ values toward COX-2 in the submicromolar concentration (with the only exception of (+)-**10b**, Table 1), while compounds were all inactive toward COX-1 at the maximum tested dose (100 μM).

All the new compounds showed a very good activity, even though, in general they are less active than corresponding previously synthesized derivatives lacking a stereogenic center at the α-position of the side chain.[23,24]

Regarding the influence of the alcohol and ether groups on activity, a comparison of racemates or corresponding enantiomers of compounds **10a** and **11a** revealed comparable IC$_{50}$ values, while less than a 2-fold difference was the maximum value found between compounds **10c** and **11c**. The major variation in affinity was found comparing (+)-**10b** and (+)-**11b** (1.10 vs 0.25 μM), and (−)-**10b** and (−)-**11b** (0.075 vs 0.81 μM), while their racemates **10b** and **11b** showed very similar activity (0.12 vs 0.10 μM, respectively).

Analysis of the influence of the substituent on the N1 phenyl ring showed that ether derivatives **11a** and **11c** (both racemates and enantiomers) were characterized by comparable IC$_{50}$ values, while the 3-F derivatives (+)- and (−)-**11b** were slightly less active. All of the alcohol derivatives had a good biological profile in terms of both IC$_{50}$ values and percent inhibition values. In fact, COX-2 affinity was ranging from 0.075 through 0.30 μM, and COX-2 percent inhibition was higher than 92% (at a 10 μM dose), with the exception of (+)-**10b** (IC$_{50}$ 1.10 μM, 84% enzyme inhibition).

Compound (+/−)-**10b** was submitted to further pharmacological tests. In particular, the HWB assay was performed to evaluate the actual extent of isozyme inhibition achievable in vivo by circulating drug levels, because of a number of variables potentially affecting inhibitor–enzyme interaction. Results indicated that

compound (+/−)-**10b** had a comparable COX-2 selectivity to **2** while it was about 5-fold less selective than **1b** (the selectivity index, expressed as COX-1/COX-2 IC$_{50}$ ratio, was 5.6, 4.9, and 29.6, respectively, Fig. 1A–C). Differently, in the in vitro cell-based assay, **1b** showed a selectivity index of about 62, lower than that found for (+/−)-**10b** (>300). The discrepancy of these results could be due to several matters. In particular, the use of exogenous arachidonic acid (AA) in the assay for COX-1 activity in vitro, in murine monocyte/macrophage J774 cell line, might have caused a loss in COX-1 affinity for an AA-dependent allosteric activation of COX-1, which induces a conformational change in the enzyme binding site.[27]

The same compound was also checked for its in vivo anti-inflammatory (carrageenan-induced paw edema test) and analgesic (paw-pressure test and abdominal writhing test) activity. Thirty minutes after a 20 mg/kg po administration, it showed a good activity against carrageenan-induced hyperalgesia (paw-pressure test, Table 2), very similar to that obtained with **1b** (10 mg/kg po). However, different from what was observed with **1b**, the activity tended to fade at longer time-points (60 min), disappearing al-
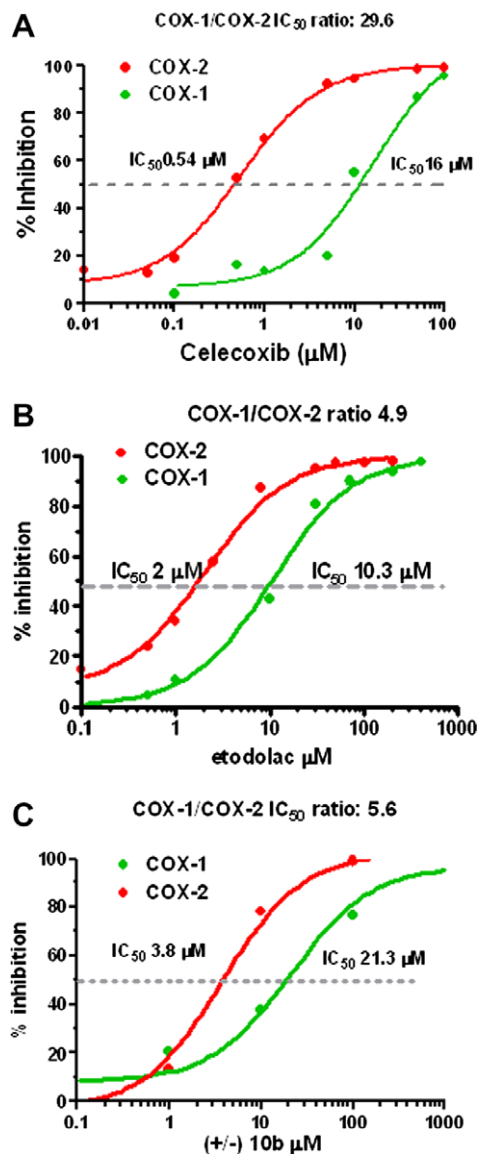

Figure 1. In vitro inhibition (human whole blood assay) of COX-1 and COX-2 by **1b** (A), **2** (B), and (+/−)-**10b** (C).

Table 2
Effect of (+/−)-**10b** in the rat paw-pressure test, in comparison to **1b**[a]

Pre-treatment	Treatment	Paw pressure (g)			
		Before pre-treatment	After treatment (min)		
			30	60	120
Saline	Saline	63.4 ± 4.6	60.2 ± 5.1	62.9 ± 4.9	60.7 ± 5.4
Carrageenan	Saline	61.9 ± 5.1	38.7 ± 5.3	35.8 ± 4.5	40.1 ± 5.0
Carrageenan	(+/−)-**10b**	59.6 ± 2.8	54.8 ± 3.8[*]	45.2 ± 4.6	47.5 ± 4.6
Carrageenan	**1b**	62.7 ± 3.9	56.5 ± 3.8[*]	58.2 ± 4.4[*]	55.2 ± 5.1[*]

[a] (+/−)-**10b** and **1b** were administered at the dose of 20 and 10 mg/kg po, respectively.
[*] $P < 0.01$ versus carrageenan/saline-treated group.

Table 3
Effect of compounds (+/−)-**10b** and **1b** in the edema induced by carrageenan[a]

Pre-treatment	Treatment	Paw volume (mL)	
		Before pre-treatment	60 min after treatment
Saline	Saline	1.25 ± 0.09	1.29 ± 0.10
Carrageenan	Saline	1.22 ± 0.08	2.33 ± 0.08
Carrageenan	(+/−)-**10b**	1.37 ± 0.12	1.40 ± 0.13[*]
Carrageenan	**1b**	1.28 ± 0.14	1.33 ± 0.10[*]

[a] (+/−)-**10b** and **1b** were administered at the dose of 20 and 10 mg/kg po, respectively.
[*] $P < 0.01$ versus carrageenan/saline-treated group.

most completely 120 min after administration. In parallel, a good activity was demonstrated against carrageenan-induced edema in the rat paw (Table 3), with a complete remission 60 min after the administration (20 mg/kg po). Moreover, a dose-dependent antinociceptive activity was observed in the abdominal writing test (Table 4).

2.4. Computational studies on the binding mode

Following a computational protocol previously described,[23] molecular docking simulations (software Autodock 3.0)[28] were performed on the enantiomeric pairs of alcohol derivatives **10b** and **10c**, as well as on the enantiomers of the ether derivative **11b**. Results of calculations showed that all the compounds assumed the same orientation within the COX-2 binding site, with the methylsulfonyl group located into the selectivity site (according to the notation used by Kurumbail et al.),[29] the 5-phenyl ring accommodated into the hydrophobic pocket, and the side chain at position 3 of the pyrrole ring matching the carboxylate site (Fig. 2A). In further detail, the best docked conformation of (−)-(R)-**10b**, belonging to the first ranked and most populated docking cluster, was also characterized by expected features. In fact, its fluorine substituent was located at close contact with the portion of the hydrophobic pocket previously identified by Grid[30] as the best interaction region for the fluoride probe.[23,24] Moreover, the methyl group at position 2 of the pyrrole approximately corresponded to one of the profitable interac-

Table 4
Effect of compound (+/−)-**10b** in the mouse abdominal writhing test (acetic acid 0.6%)

Treatment[a]	Number of mice	Dose (po mg kg⁻¹)	Number or writhes
CMC	25		38.1 ± 2.6
(+/−)-**10b**	8	10	26.3 ± 3.6
(+/−)-**10b**	8	20	16.1 ± 2.7[*]

[a] All compounds were administered per os 30 min before test.
[*] $P < 0.01$ versus vehicle-treated mice.

tion points for the methyl probe, while the carbonyl oxygen of the ester moiety occupied a pocket (close to the terminal portion of the Arg120 side chain) identified by the carbonyl probe of Grid. As a consequence, also in terms of interactions with the COX-2 binding site, (−)-(R)-**10b** made expected contacts (Fig. 2A). In fact, one of the sulfone oxygens interacted by a hydrogen bond with the NH group of Tyr518, while the carbonyl oxygen contacted the basic portion of Arg120. A very similar orientation and interactions were also found for the corresponding S-enantiomer of **10b**, with only a major difference involving the alcohol group (Fig. 2B). In particular, in the case of the S-enantiomer, such a residue was directed toward a large hydrophobic region delimited by Val349, Leu359, and Leu531, without any interaction with the protein. Differently, the same group of the R-enantiomer pointed toward Ser353 and made an additional hydrogen bond contact with its hydroxy group, probably accounting for the higher affinity of the R-enantiomer in comparison to the S-enantiomer. Moreover, the N1 phenyl ring of the S-enantiomer underwent a conformational rearrangement (Fig. 2B), in comparison with the same moiety of the R-enantiomer, leading the fluorine substituent in a region of space not perfectly corresponding to the profitable interaction point found by Grid for the fluorine probe.

Transforming **10b** into the corresponding ethyl ether derivative **11b**, the overall orientation within the binding site remained quite unaltered (Fig. 3). Moreover, enantiomers of **11b** showed a very similar pose (in both cases, we chose the first conformation of the first ranked cluster, corresponding to the most populated docking cluster) also in terms of orientation of the side chain at position 3 of the pyrrole. In fact, the ether side chain of both enantiomers was located within the hydrophobic region defined by Val349, Leu359, and Leu531 and pointed toward Ile345, while the ester portions were accommodated within the carboxylate site. The only difference was that the S-enantiomer contacted with its carbonyl oxygen the terminal part of Arg120 side chain, accordingly to Grid simulations for the oxygen probe. Differently, the ether oxygen of the ester moiety of the R-enantiomer was able to make a hydrogen bond with the same residue. However, such an oxygen atom was located in a region quite far from the pocket identified by Grid for profitable interactions with Arg120, accounting for the decreased affinity (about 3-fold) with respect to S-enantiomer.

Regarding the p-methoxy derivative **10c**, its R-enantiomer showed a binding mode and interactions with the protein very similar to (−)-(R)-**10b**. As a consequence, although additional hydrophobic contacts involving the methoxy group and the hydrophobic region of the protein were found, affinity of (−)-(R)-**10c** was comparable to that of (−)-(R)-**10b**. On the other hand, (+)-(S)-**10c**, whose hydroxy group lacked the contact with Ser353, showed an unexpected high affinity for the enzyme. However, it gained van der Waals interactions by means of its terminal methyl group (part of the p-methoxy substituent) that was able to fill a hydrophobic cavity defined by Phe381, Leu384, and Tyr385 (Fig. 4).

In summary, docking simulations showed that the new chiral derivatives adopted a binding mode very similar to that previously reported for the corresponding achiral parent compounds, in terms of both orientation within the binding site and interactions with the protein. Hydrogen bonds involving the sulfonyl oxygens and the carbonyl group of the ligands, which interacted with Tyr518 and Arg120, respectively, were confirmed as important anchor points for the binding of COX-2 inhibitors. Moreover, additional interactions, such as a hydrogen bond with Ser353 and van der Waals contacts with the hydrophobic region, could serve to modulate affinity of compounds toward the enzyme.
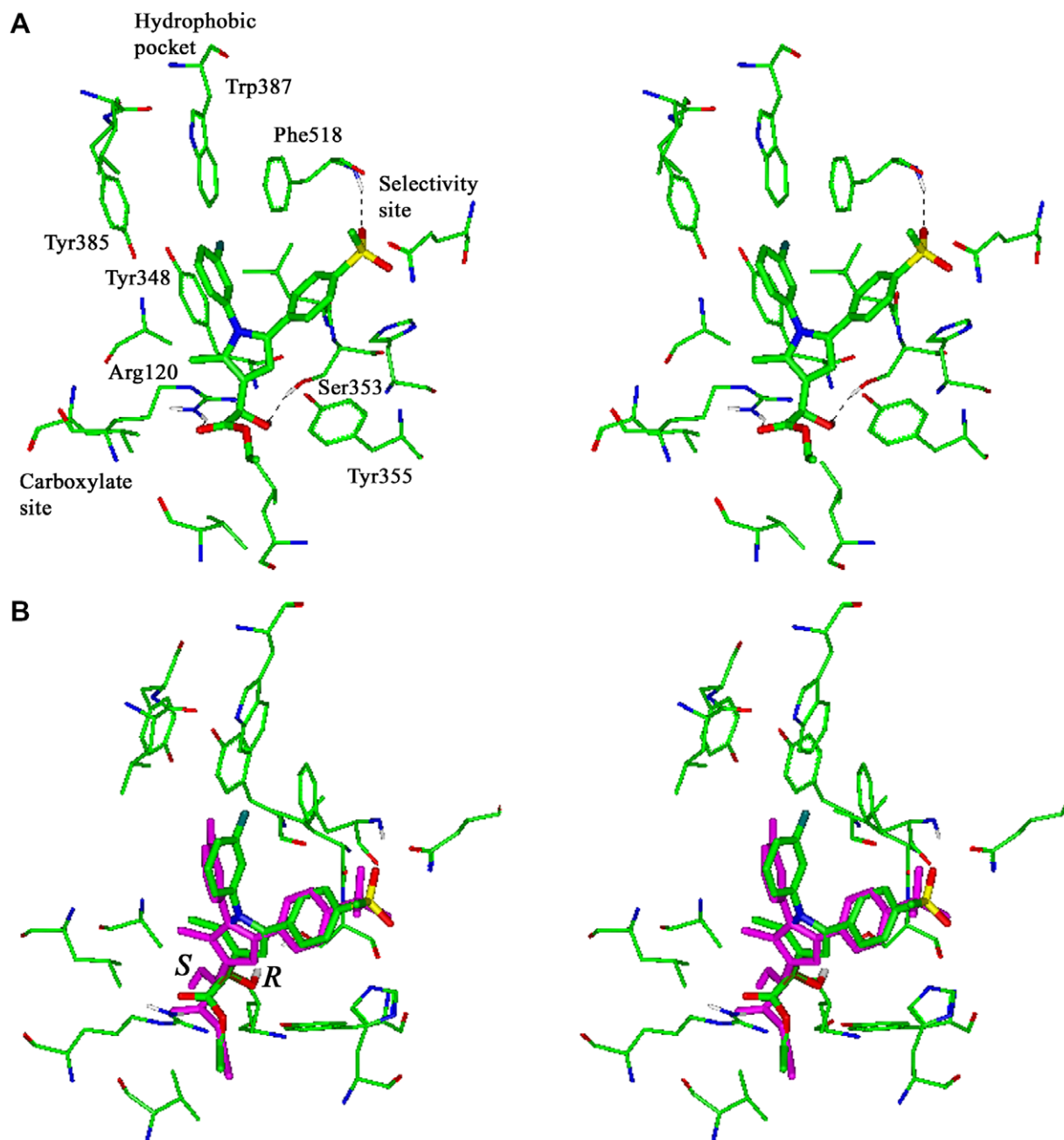
Figure 2. (A) Stereographical representation of the binding mode of (−)-*R*-**10b**, taken as the representative compound of the new pyrrole derivatives, into the binding pocket of COX-2. Hydrogen bonds involving the inhibitor and Arg120, Ser353, and Phe518, are shown as black dashed lines. (B) Stereographical representation of the binding mode of (−)-*R*-**10b** (green, thick lines) and (+)-*S*-**10b** (magenta, thick lines). The major difference involves the orientation of the hydroxy group on the stereogenic center. A conformational rearrangement also occurs in the N1 phenyl ring of the *S*-enantiomer with respect to the corresponding *R*-enantiomer.

3. Experimental

3.1. Chemistry

All chemicals used were of reagent grade. Yields refer to purified products, and are not optimized. Melting points were determined in open capillaries on a Gallenkamp apparatus, and are uncorrected. Microanalyses were carried out by means of a Perkin-Elmer 240 C or a Perkin-Elmer Series II CHNS/O Analyzer 2400. Merck silica gel 60 (230–400 mesh) was used for column chromatography. Merck TLC plates, silica gel 60 F_{254}, were used for TLC. ^{1}H NMR spectra were recorded with a Bruker AC 200 spectrometer in the indicated solvent (TMS as internal standard).

The values of the chemical shifts are expressed in ppm and the coupling constants (*J*) in Hertz. Mass spectra were recorded on either a Varian Saturn 3 or a ThermoFinnigan LCQ-deca spectrometer.

3.2. Preparation of ethyl 1,5-diarylpyrrol-3-ylglyoxylic esters (12a–c)

These compounds were prepared starting from the corresponding 1,5-diaryl-2-methylpyrroles, by regioselective acylation (at position 3) with ethoxalyl chloride in the presence of pyridine. Analytical data, mp, and ^{1}H NMR spectra were consistent with those reported in the literature.[23,24]
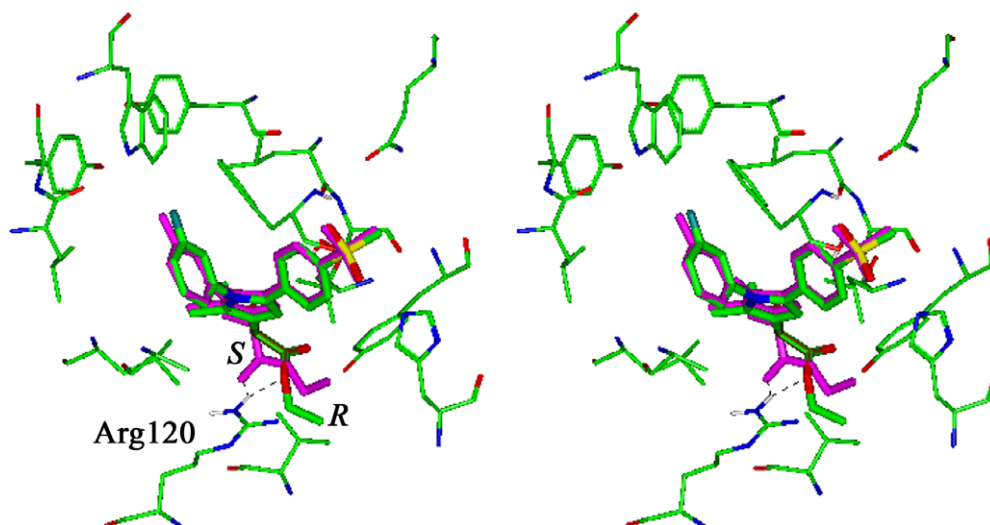
Figure 3. Stereographical representation of the binding mode of (−)-R-**11b** (green, thick lines) and (+)-S-**11b** (magenta, thick lines) showing the different hydrogen bonding patterns: the terminal portion of Arg120 side chain interacts with the carbonyl oxygen of the S-enantiomer, as well as with the ether oxygen of the ester chain of the R-enantiomer.

Analytical data

Compound	Formula	C Calcd % Found%	H Calcd% Found%	N Calcd% Found%
10a	$C_{22}H_{23}NO_5S$	63.90 63.95	5.61 4.57	3.39 3.40
10b	$C_{22}H_{22}FNO_5S$	61.24 61.22	5.14 5.10	4.40 4.45
10c	$C_{23}H_{25}NO_6S$	62.29 62.30	5.68 5.65	3.16 3.18
11a	$C_{23}H_{25}NO_5S$	64.62 64.58	5.89 5.90	3.28 3.22
11b	$C_{23}H_{24}FNO_5S$	62.01 62.00	5.43 5.40	4.26 4.20
11c	$C_{24}H_{27}NO_6S$	63.00 63.02	5.65 5.63	3.06 3.00

3.3. General procedure for the preparation of 1,5-diarylpyrrole-3-(α-hydroxy) acetic esters (10a–c)

To a solution of the appropriate ethyl 1,5-diarylpyrrol-3-ylglyoxylic ester **12a–c** (1.46 mmol) in CH_2Cl_2 (9 mL) stirred at rt, ZnI_2 (0.67 g, 2.17 mmol) was added. Sodium cyanoborohydride (0.07 g, 1.08 mmol) was added after 5 min, the mixture was left to react for 2 h, under nitrogen atmosphere, stirring at rt. At the end, tert-butyl alcohol (100 mL) was added. The mixture was filtered on Celite and the solution obtained was acidified with a solution of ammonium chloride (10%) in HCl 6 N and extracted with $CHCl_3$. The organic solution was washed, dried, and evaporated in vacuo. The resulting residue was chromatographed on silica gel eluting with ether/ethyl acetate (1:1) to give a solid, which, after re-crystallization from ethyl acetate, afforded the required product. Enantiomers of each compound described have been separated by chromatography, using a Chiral Pack IA, chiral stationary phase, with n-hexane/CH_2Cl_2/ethanol (50:50:1) as the eluant.

3.3.1. Ethyl-[2-hydroxy-2-[2-methyl-5-(4-methylsulfonyl)-phenyl-1-phenyl-1H-pyrrol-3-yl]]acetate (10a)

Mp 145 °C (0.30 g, yield 50%); ^1H NMR (CDCl$_3$) 7.62–7.67 (m, 2H), 7.24–7.27 (m, 3H), 7.12–7.17 (m, 4H), 6.47–6.50 (m, 1H), 5.21 (s, 1H), 4.24–4.37 (m, 2H), 3.20–3.22 (br, 1H), 2.96–3.01 (s, 3H), 2.13–2.18 (s, 3H), 1.28–1.35 (t, 3H). Anal. ($C_{22}H_{23}NO_5S$) C, H, N.

(+)-(S)-Ethyl-[2-hydroxy-2-[2-methyl-5-(4-methylsulfonyl)phenyl-1-phenyl-1H-pyrrol-3-yl]]acetate ((+)-(S)-**10a**). $[\alpha]_D$ +70° (c 0.049, EtOH).

(−)-(R)-Ethyl-[2-hydroxy-2-[2-methyl-5-(4-methylsulfonyl)phenyl-1-phenyl-1H-pyrrol-3-yl]]acetate. (−)-(R)-**10a**. $[\alpha]_D$ −60° (c 0.049, EtOH).

3.3.2. Ethyl-[2-hydroxy-2-[1-(3-fluoro)phenyl-2-methyl-5-(4-methylsulfonyl)phenyl-1H-pyrrol-3-yl]]acetate (10b)

Mp 173 °C (0.315 g, yield 50%); ^1H NMR (CDCl$_3$): 7.66–7.72 (d, 2H), 7.37–7.38 (m, 1H), 7.24–7.25 (d, 2H), 6.90–6.93 (m, 3H), 6.46–6.47 (s, 1H), 5.18 (s, 1H), 4.22–4.35 (m, 2H), 2.99–3.20 (br, 1H) 2.98 (s, 3H), 2.15 (s, 3H), 1.24–1.32 (m, 3H). Anal. ($C_{22}H_{22}FNO_5S$) C, H, N.

(+)-(S)-Ethyl-[2-hydroxy-2-[1-(3-fluoro)phenyl-2-methyl-5-(4-methylsulfonyl)phenyl-1H-pyrrol-3-yl]]acetate ((+)-(S)-**10b**). $[\alpha]_D$ +88° (c 0.019, EtOH).

(−)-(R)-Ethyl-[2-hydroxy-2-[1-(3-fluoro)phenyl-2-methyl-5-(4-methylsulfonyl)phenyl-1H-pyrrol-3-yl]]acetate ((−)-(R)-**10b**). $[\alpha]_D$ = −81° (c 0.046, EtOH).

3.3.3. Ethyl-[2-hydroxy-2-[1-(4-methoxy)phenyl-2-methyl-5-(4-methylsulfonyl)phenyl-1H-pyrrol-3-yl]]acetate (10c)

Mp 130 °C (0.324 g, yield 50%); ^1H NMR (CDCl$_3$): 7.65–7.67 (d, 2H), 7.16–7.18 (d, 2H), 7.12–7.15 (m, 2H), 7.06–7.11 (m, 2H), 6.46 (s, 1H), 5.02 (s, 1H), 4.19 (m, 2H), 3.85 (s, 3H), 3.20–3.25 (br, 1H), 3.00 (s, 3H), 2.14 (s, 3H), 1.29–133 (t, 3H). Anal. ($C_{23}H_{25}NO_6S$) C, H, N.

(+)-(S)-Ethyl-[2-hydroxy-2-[1-(4-methoxy)phenyl-2-methyl-5-(4-methylsulfonyl)phenyl-1H-pyrrol-3-yl]]acetate ((+)-(S)-**10c**). $[\alpha]_D$ +57° (c 0.086, EtOH).

(−)-(R)-Ethyl-[2-hydroxy-2-[1-(4-methoxy)phenyl-2-methyl-5-(4-methylsulfonyl)phenyl-1H-pyrrol-3-yl]]acetate ((−)-(R)-**10c**). $[\alpha]_D$ −58° (c 0.091, EtOH).
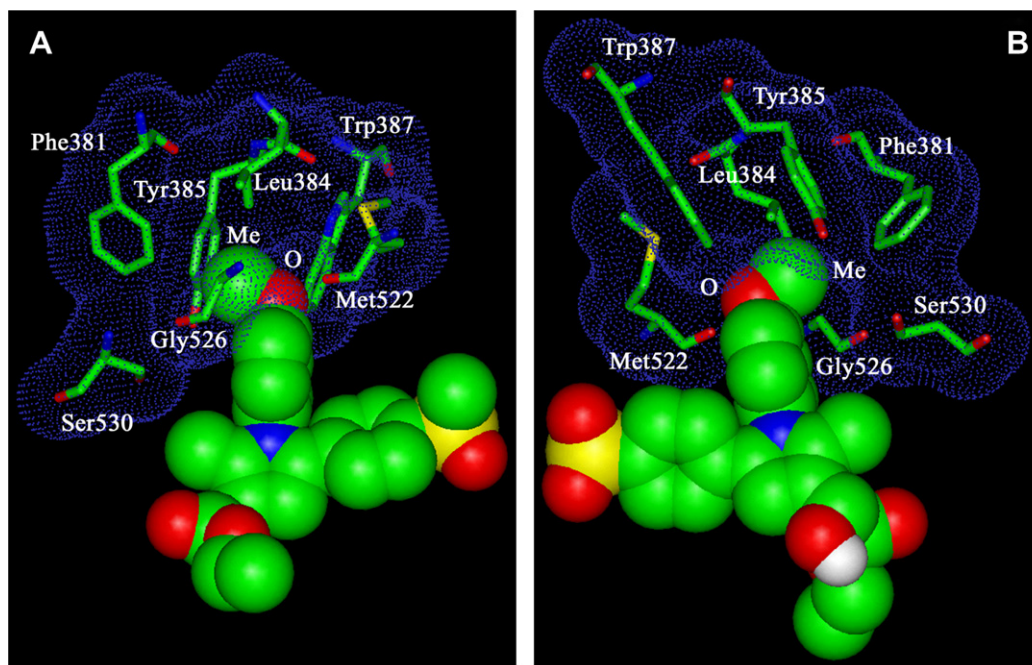
Figure 4. Graphical representation of two different views of the complex between COX-2 and (−)-*R*-**10c**. Analysis of the molecular surface of inhibitor and portion of the hydrophobic pocket of the binding site shows a perfect complementarity between hydrophobic amino acid side chains (Phe381, Tyr385, Leu384, and Trp387) and the 4-methoxy group of the inhibitor (labeled as Me for the methyl portion and as O for the oxygen atom). The picture of the left panel shows the inhibitor in an orientation comparable to that of Figure 2A, while in the right panel the complex was rotated 180° on the *Y*-axis.

3.4. General procedure for the preparation of 1,5-diarylpyrrole-3-(α-ethoxy) acetic esters (11a–c)

To a solution of the appropriate ethyl 1,5-diarylpyrrol-3-ylglyoxylic esters **12a–c** (1.46 mmol) in CH$_2$Cl$_2$ (9 mL) stirred at rt, ZnCl$_2$ (0.67 g, 2.17 mmol) was added. Sodium cyanoborohydride (0.07 g, 1.08 mmol) was added after 5 min, the mixture was left to react for 2 h, under nitrogen atmosphere, stirring at rt. At the end, ethyl alcohol (100 mL) was added. The mixture was filtered on Celite, and the solution obtained was acidified with a solution of ammonium chloride (10%) in HCl 6 N and extracted with CHCl$_3$. The organic solution was washed, dried, and evaporated in vacuo. The resulting residue was chromatographed on silica gel eluting with ether/ethyl acetate (1:1) to give a solid, which, after re-crystallization from ethyl acetate, afforded the required product. Enantiomers of the compound described were separated by chromatography, using a Chiral Pack IA, chiral stationary phase, with *n*-hexane/CH$_2$Cl$_2$/ethanol (70:25:0.2) as the eluant.

3.4.1. Ethyl-[2-ethoxy-2-[-2-methyl-5-(4-methylsulfonyl)-phenyl-1-phenyl-1*H*-pyrrol-3-yl]]acetate (11a)

Mp 165 °C (0.322 g, yield 50%); ^{1}H NMR (CDCl$_3$) 7.62–7.64 (m, 2H), 7.24–7.27 (m, 3H), 7.12–7.15 (m, 4H), 6.47–6.60 (m, 1H), 4.92 (s, 1H), 4.15–4.40 (m, 2H), 3.50–3.70 (m, 2H), 2.97–3.00 (s, 3H), 2.13–2.18 (s, 3H), 1.28–1.32 (t, 6H). Anal. (C$_{24}$H$_{27}$NO$_5$S) C, H, N.

*(+)-(S)-Ethyl-[2-ethoxy-2-[-2-methyl-5-(4-methylsulfonyl)phenyl-1-phenyl-1H-pyrrol-3-yl]]acetate ((+)-(S)-**11a**).* [α]$_D$ +41° (*c* 0.027, EtOH).

*(−)-(R)-Ethyl-[2-ethoxy-2-[-2-methyl-5-(4-methylsulfonyl)phenyl-1-phenyl-1H-pyrrol-3-yl]]acetate ((−)-(R)**11a**).* [α]$_D$ −52° (*c* 0.022, EtOH).

3.4.2. Ethyl-[2-ethoxy-2-[1-(3-fluoro)phenyl-2-methyl-5-(4-methylsulfonyl)phenyl-1*H*-pyrrol-3-yl]]acetate (11b)

Mp 165 °C (0.369 g, yield 55%); ^{1}H NMR (CDCl$_3$): 7.66–7.72 (d, 2H), 7.37–7.38 (m, 1H), 7.23–7.25 (d, 2H), 6.90–6.93 (m, 3H),

6.55–6.57 (s, 1H), 4.79–4.82 (s, 1H), 4.23–4.27 (m, 2H), 3.43–3.45 (m, 2H) 2.96–3.00 (s, 3H), 2.16 (s, 3H), 1.28–1.32 (t, 6H). Anal. (C$_{24}$H$_{26}$FNO$_5$S) C, H, N.

*(+)-(S)-Ethyl-[2-ethoxy-2-[1-(3-fluoro)phenyl-2-methyl-5-(4-methylsulfonyl)phenyl-1H-pyrrol-3-yl]]acetate ((+)-(S)-**11b**).* [α]$_D$ +45° (*c* 0.041, EtOH).

*(−)-(R)-Ethyl-[2-ethoxy-2-[1-(3-fluoro)phenyl-2-methyl-5-(4-methyl sulfonyl)phenyl-1H-pyrrol-3-yl]]acetate ((−)-(R)-**11b**).* [α]$_D$ −34° (*c* 0.020, EtOH).

3.4.3. Ethyl-[2-ethoxy-2-[1-(4-methoxy)phenyl-2-methyl-5-(4-methylsulfonyl)phenyl-1*H*-pyrrol-3-yl]]acetate (11c)

Mp 159 °C (0.344 g, yield 50%); ^{1}H NMR (CDCl$_3$): 7.65–7.67 (d, 2H), 7.14–7.16 (d, 2H), 7.04–7.08 (m, 2H), 6.88–6.90 (m, 2H), 6.56 (s, 1H), 4.89–490 (s, 1H), 4.18–4.28 (m, 2H), 3.77–3.83 (s, 3H), 3.56–3.65 (m, 2H), 2.92–2.98 (s, 3H), 2.14 (s, 3H), 1.23–131 (t, 6H). Anal. (C$_{25}$H$_{29}$NO$_6$S) C, H, N.

*(+)-(S)-Ethyl-[2-ethoxy-2-[1-(4-methoxy)phenyl-2-methyl-5-(4-methylsulfonyl)phenyl-1H-pyrrol-3-yl]]acetate ((+)-(S)-**11c**).* [α]$_D$ +32° (*c* 0.040, EtOH).

*(−)-(R)-Ethyl-[2-ethoxy-2-[1-(4-methoxy)phenyl-2-methyl-5-(4-methylsulfonyl)phenyl-1H-pyrrol-3-yl]]acetate ((−)-(R)-**11c**).* [α]$_D$ −43° (*c* 0.043, EtOH).

3.5. Biology

Arachidonic acid was obtained from SPIBIO (Paris, France). [^{3}H]PGE$_2$ and [^{3}H]TXB$_2$ were from Perkin-Elmer Life Sciences (Milan, Italy). Compound **1b** was kindly provided by Merck (Darmstadt, Germany), **2** and all other reagents and compounds used were obtained from Sigma–Aldrich (Milan, Italy).

3.5.1. Cellular assay

3.5.1.1. Cell culture. The murine monocyte/macrophage J774 cell line was grown in Dulbecco's modified Eagle's medium (DMEM) supplemented with 2 mM glutamine, 25 mM Hepes, penicillin (100 U/mL), streptomycin (100 µg/mL), 10% fetal bovine serum

(FBS), and 1.2% sodium pyruvate (Bio Whittaker, Europe). Cells were plated in 24-well culture plates at a density of 2.5×10^5 cells/mL or in 10 cm-diameter culture dishes (1×10^7 cells/10 mL/dish) and were allowed to adhere at 37 °C in 5% CO_2/95% O_2 for 2 h. Immediately before the experiments, the culture medium was replaced by a fresh medium without FBS in order to avoid interference with radioimmunoassay,[31] and cells were stimulated as described.

3.5.1.2. Assessment of COX-1 activity. Cells were pre-treated with the reference standard (**1b**) or the test compounds (0.01–100 μM) for 15 min, and were further incubated at 37 °C for 30 min with 15 μM arachidonic acid in order to activate the constitutive COX.[31] Stock solutions of the reference standard or of the test compounds were prepared in dimethyl sulfoxide, and an equivalent amount of dimethyl sulfoxide was included in control samples. At the end of the incubation, the supernatants were collected for the measurement of PGE_2 levels by radioimmunoassay.

3.5.1.3. Assessment of COX-2 activity. Cells were stimulated for 24 h with *Escherichia coli* lipopolysaccharide (LPS, 10 μg/mL) to induce COX-2, in the absence or in the presence of test compounds, at the concentrations previously reported. The supernatants were collected for the measurement of PGE_2 levels by radioimmunoassay.

3.5.1.4. Statistical analysis. Triplicate wells were used for the various conditions of treatment. Results are expressed as the mean, for three experiments, of the percent inhibition of PGE_2 production by test compounds with respect to control samples. Data fit was obtained using the sigmoidal dose–response equation (variable slope) (GraphPad software).

3.5.2. Human whole blood (HWB) assay
3.5.2.1. Subjects. Three healthy volunteers (2 female and 1 male, aged 29 ± 3 years) were enrolled to participate in the study after its approval by the Ethical Committee of the University of Chieti. Informed consent was obtained from each subject.

3.5.2.2. COX-2 assay. To evaluate COX-2 activity, 1 mL aliquots of peripheral venous blood samples containing 10 iu of sodium heparin were incubated in the presence of LPS (10 μg/mL) or saline for 24 h at 37 °C as previously described.[5] The contribution of platelet COX-1 was suppressed by pre-treating the subjects with aspirin (300 mg, 48 h) before sampling. Plasma was separated by centrifugation (10 min at 2000 rpm), and was kept at −80 °C until assayed by RIA for PGE_2, as an index of LPS-induced monocyte COX-2 activity.

3.5.2.3. COX-1 assay. Peripheral venous blood samples were drawn from the same donors when they had not taken any NSAID during the 2 weeks preceding the study. One-milliliter aliquots of whole blood were immediately transferred into glass tubes, and were allowed to clot at 37 °C for 1 h. Serum was separated by centrifugation (10 min at 3000 rpm), and was kept at −80 °C until assayed for TXB_2. Whole blood TXB_2 production was measured by RIA as a reflection of maximally stimulated platelet COX-1 activity in response to endogenously formed thrombin.[32]

3.5.2.4. Effects of COX-2 Inhibitors on whole blood COX-2 and COX-1 activities. Compounds **1b** (0.005–50 mM), **2** (0.005–200 mM), and **10b** (0.5–50 mM) were dissolved in DMSO. Aliquots of the solutions (2 μL) were pipetted directly into test tubes to give final concentrations of 0.01–100 μM in heparinized whole blood samples in the presence of LPS (10 μg/mL) for 24 h or with whole blood samples allowed to clot at 37 °C for 1 h, in order to examine the concentration-dependence of COX-2 versus COX-1 inhibition, respectively.

3.5.2.5. Analysis of PGE_2 and TXB_2. PGE_2 and TXB_2 concentrations were measured by previously described and validated radioimmunoassays.[5,32] Unextracted plasma and serum samples were diluted in the standard diluent of the assay (0.02 M phosphate buffer, pH 7.4), and were assayed in a volume of 1.5 mL at a final dilution of 1:50–1:30,000. [^{3}H]PGE_2 or [^{3}H]TXB_2 (4000 dpm, specific activity >100 Ci/mmol, Perkin-Elmer Life Science Products, Brussels, Belgium) and specific anti-PGE_2 (1:100,000 dilution) and anti-TXB_2 (1:120,000 dilution) sera were used. The least detectable concentration was 1–2 pg/mL for both prostanoids.

3.5.2.6. Statistical analysis. Results are expressed as the mean, for three experiments (triplicate wells were used for the various conditions of treatment, in the cell culture assay), of the percent inhibition of prostanoid production assessed in the absence of the test compounds (control). Concentration–response curves were fitted, and IC_{50} values were analyzed with PRISM (Graph-Pad, San Diego, CA, USA) and ALLFIT, a basic computer program for simultaneous curve-fitting based on a four-parameter logistic equation.

3.5.3. In vivo anti-inflammatory activity
3.5.3.1. Animals. Male Swiss albino mice (23–25 g) and Sprague–Dawley or Wistar rats (150–200 g) were used. Fifteen mice and four rats were housed per cage. The cages were placed in the experimental room 24 h before the test for acclimatization. The animals were fed in a standard laboratory diet and tap water ad libitum, and were kept at 23 ± 1 °C with a 12 h light/dark cycle, light on at 7 am. All experiments were carried out in accordance with the NIH Guide for the Care and Use of Laboratory animals. All efforts were made to minimize animal suffering, and to reduce the number of animals used.

3.5.3.2. Paw-pressure test. The nociceptive threshold in the rat was determined with an analgesimeter, according to the method described by Leighton.[33] Threshold pressure was measured before and 30, 60, and 120 min after treatment. An arbitrary cut-off value of 250 g was adopted. In order to induce an inflammatory process in the rat, paw carrageenan (0.1 mL, 1%) was administered ip 4 h before test.

3.5.3.3. Carrageenan-induced paw edema. Rat paw volumes were measured using a plethysmometer. Five hours after the injection of carrageenan (0.1 mL injection of 1.0%) the paw volume of the right hind paw was measured and compared with saline/carrageenan-treated controls.[34] Rats received test compounds 4 h after carrageenan. Results are reported as paw volume expressed in milliliter.

3.5.3.4. Abdominal writhing test. Mice were injected ip with a 0.6% solution of acetic acid (10 mL/kg), according to Koster.[35] The number of stretching movements was counted for 10 min, starting 5 min after acetic acid injection.

Acknowledgment

References

1. Burke, A.; Smyth, E.; FitzGerald, G. A. In *The Pharmacological Basis of Therapeutics*; Brunton, L. L., Lazo, J. S., Parker, K. L., Eds., 11th ed.; Autacoids: Drug Therapy Of Inflammation; Macmillan Publishing Co.: New York, 2005; pp 671–736. Section IV.
2. FitzGerald, G. A.; Patrono, C. *N. Engl. J. Med.* **2001**, *345*, 433.
3. Grosser, T.; Fries, S.; FitzGerald, G. A. *J. Clin. Invest.* **2006**, *116*, 4.

4. Capone, M. L.; Tacconelli, S.; Di Francesco, L.; Sacchetti, A.; Sciulli, M. G.; Patrignani, P. *Prostaglandins Other Lipid Mediat.* **2007**, *82*, 85.
5. Patrignani, P.; Panara, M. R.; Greco, A.; Fusco, O.; Natoli, C.; Iacobelli, S.; Cipollone, F.; Ganci, A.; Crèminon, C.; Maclouf, J.; Patrono, C. *J. Pharmacol. Exp. Ther.* **1994**, *271*, 1705.
6. Patrignani, P.; Panara, M. R.; Sciulli, M. G.; Santini, G.; Renda, G.; Patrono, C. *J. Physiol. Pharmacol.* **1997**, *48*, 623.
7. Ferdinandi, E. S.; Cayen, M. N.; Pace-Asciak, C. *J. Pharmacol. Exp. Ther.* **1982**, *220*, 417.
8. Engelhardt, G.; Homma, D.; Schlegel, K.; Utzmann, R.; Schnitzler, C. *Inflamm. Res.* **1995**, *44*, 423.
9. Weissenbach, R. *J. Int. Med. Res.* **1981**, *9*, 349.
10. Ku, E. C.; Wasvary, J. M.; Cash, W. D. *Biochem. Pharmacol.* **1975**, *24*, 641.
11. Prasit, P.; Wang, Z.; Brideau, C.; Chan, C. C.; Charleson, S.; Cromlish, W.; Ethier, D.; Evans, J. F.; Ford-Hutchinson, A. W.; Gauthier, J. Y.; Gordon, R.; Guay, J.; Gresser, M.; Kargman, S.; Kennedy, B.; Leblanc, Y.; Leger, S.; Mancini, J.; O'Neill, G. P.; Quellet, M.; Percival, M. D.; Perrier, H.; Riendeau, D.; Rodger, I.; Tagari, P.; Therien, M.; Vickers, P.; Wong, E.; Xu, L. J.; Young, R. N.; Zamboni, R.; Boyce, S.; Rupniak, N.; Forrest, M.; Visco, D.; Patrick, D. *Bioorg. Med. Chem. Lett.* **1999**, *9*, 1773.
12. Penning, T. D.; Tally, J. J.; Bertenshaw, S. R.; Carter, J. S.; Collins, P. W.; Doctor, S.; Graneto, M. J.; Lee, L. F.; Malecha, J. W.; Miyashiro, J. M.; Rogers, R. S.; Rogier, D. J.; Yu, S. S.; Anderson, G. D.; Burton, E. G.; Cogburn, J. N.; Gregory, S. A.; Koboldt, C. M.; Perkins, W. E.; Seibert, K.; Veenhuizen, A. W.; Zhang, Y. Y.; Isakson, P. C. *J. Med. Chem.* **1997**, *40*, 1347.
13. Talley, J. A.; Brown, D. L.; Carter, J. S.; Masferrer, M. J.; Perkins, W. E.; Rogers, R. S.; Shaffer, A. F.; Zhang, Y. Y.; Zweifel, B. S.; Seiberk, K. *J. Med. Chem.* **2000**, *43*, 775.
14. Riendeau, D.; Percival, M. D.; Brideau, C.; Charleson, S.; Dube, D.; Ethier, D.; Falgueyret, J.-P.; Friesen, R. W.; Gordon, R.; Greig, G.; Guay, I.; Manacini, J.; Ouellet, M.; Wong, E.; Xu, L.; Boyce, S.; Visco, D.; Girad, Y.; Prasit, P.; Zamboni, R.; Rodger, J. W.; Gresser, M.; Ford-Hutchinson, A. W.; Young, R. N.; Chan, C.-C. *J. Pharmacol. Exp. Ther.* **2001**, *296*, 558.
15. Ding, C.; Jones, G. *Drugs* **2002**, *5*, 1168.
16. Fries, S.; Grosser, T.; Price, T. S.; Lawson, J. A.; Kapoor, S.; DeMarco, S.; Pletcher, M. T.; Wiltshire, T.; FitzGerald, G. A. *Gastroenterology* **2006**, *130*, 55.
17. Huntjens, D. R.; Danhof, M.; Della Pasqua, O. E. *Rheumatology (Oxford)* **2005**, *44*, 846.
18. Roszkowski, A. P.; Rooks, W. H., 2nd; Tomolonis, A. J.; Miller, L. M. *J. Pharmacol. Exp. Ther.* **1971**, *179*, 114.
19. Capone, M. L.; Tacconelli, S.; Sciulli, M. G.; Grana, M.; Ricciotti, E.; Minuz, P.; Di Gregorio, P.; Merciaro, G.; Patrono, C.; Patrignani, P. *Circulation* **2004**, *109*, 1468.
20. Capone, M. L.; Tacconelli, S.; Sciulli, M. G.; Anzellotti, P.; Di Francesco, L.; Merciaro, G.; Di Gregorio, P.; Patrignani, P. *J. Pharmacol. Exp. Ther.* **2007**, *322*, 453.
21. Hernandez-Diaz, S.; Varas-Lorenzo, C.; Garcia Rodriguez, L. A. *Basic Clin. Pharmacol. Toxicol.* **2006**, *98*, 266.
22. Kearney, P. M.; Baigent, C.; Godwin, J.; Halls, H.; Emberson, J. R.; Patrono, C. *Brit. Med. J.* **2006**, *332*, 1302.
23. Biava, M.; Porretta, G. C.; Cappelli, A.; Vomero, S.; Botta, M.; Manetti, F.; Giorni, G.; Sautebin, L.; Rossi, A.; Makovec, F.; Anzini, M. *J. Med. Chem.* **2005**, *48*, 3428.
24. Biava, M.; Porretta, G. C.; Poce, G.; Supino, S.; Forli, S.; Rovini, M.; Cappelli, A.; Manetti, F.; Botta, M.; Sautebin, L.; Rossi, A.; Pergola, C.; Ghelardini, C.; Vivoli, E.; Makovec, F.; Anzellotti, P.; Patrignani, P.; Anzini, M. *J. Med. Chem.* **2007**, *50*, 5403.
25. Winter, C. A.; Risley, E. A.; Nuss, G. W. *J. Pharmacol. Exp. Ther.* **1963**, *141*, 369.
26. Biava, M.; Cirilli, R.; Fares, V.; Ferretti, R.; Gallinella, B.; La Torre, F.; Poce, G.; Porretta, G. C.; Supino, S.; Villani, C. *Chirality* **2008**, *20*, 775.
27. Swinney, D. C.; Mak, A. Y.; Barnett, J.; Ramesha, C. S. *J. Biol. Chem.* **1997**, *272*, 12393.
28. Morris, G. M.; Goodsell, D. S.; Halliday, R. S.; Huey, R.; Hart, W. E.; Belew, R. K.; Olson, A. J. *J. Comput. Chem.* **1998**, *19*, 1639.
29. Kurumbail, R. G.; Stevens, A. M.; Gierse, J. K.; McDonald, J. J.; Stegeman, R. A.; Pak, J. Y.; Gildehaus, D.; Miyashiro, J. M.; Penning, T. D.; Seibert, K.; Isakson, P. C.; Stallings, W. C. *Nature* **1996**, *384*, 644.
30. Grid, version 21, Molecular Discovery Ltd, Marsh Road, Pinner, Middlesex, UK.
31. Zingarelli, B.; Southan, G. J.; Gilad, E.; O'Connor, M.; Salzman, A. L.; Szabò, C. *Brit. J. Pharmacol.* **1997**, *120*, 357.
32. Patrono, C.; Ciabattoni, G.; Pinca, E.; Pugliese, F.; Castrucci, G.; De Salvo, A.; Satta, M. A.; Peskar, B. A. *Thromb. Res.* **1980**, *17*, 317.
33. Leighton, G. E.; Rodriguez, R. E.; Hill, R. G.; Hughes, J. *Br. J. Pharmacol.* **1988**, *93*, 553.
34. Sluka, A. K.; Westlund, K. N. *Pain* **1993**, *55*, 367.
35. Koster, R.; Anderson, M.; de Beer, E. J. *Fed. Proc.* **1959**, *18*, 412.